Chin. Geogra. Sci. 2017 Vol. 27 No. 4 pp. 539–551
doi: 10.1007/s11769-017-0886-6

Springer Science Press
www.springerlink.com/content/1002-0063

Effects of Environmental Conditions and Aboveground Biomass on CO_2 Budget in *Phragmites australis* Wetland of Jiaozhou Bay, China

GAO Manyu, KONG Fanlong, XI Min, LI Yue, LI Jihua

(*College of Environmental Science and Engineering*, *Qingdao University*, *Qingdao* 266071, *China*)

Abstract: Estuarial saline wetlands have been recognized as a vital role in CO_2 cycling. However, insufficient attention has been paid to estimating CO_2 fluxes from estuarial saline wetlands. In this study, the static chamber-gas chromatography (GC) method was used to quantify CO_2 budget of an estuarial saline reed (*Phragmites australis*) wetland in Jiaozhou Bay in Qingdao City of Shandong Province, China during the reed growing season (May to October) in 2014. The CO_2 budget study involved net ecosystem CO_2 exchange (NEE), ecosystem respiration (R_{eco}) and gross primary production (GPP). Temporal variation in CO_2 budget and the impact of air/soil temperature, illumination intensity and aboveground biomass exerted on CO_2 budget were analyzed. Results indicated that the wetland was acting as a net sink of 1129.16 g/m^{2}during the entire growing season. Moreover, the values of R_{eco} and GPP were 1744.89 g/m^2 and 2874.05 g/m^2, respectively; the ratio of R_{eco} and GPP was 0.61. Diurnal and monthly patterns of CO_2 budget varied significantly during the study period. R_{eco} showed exponential relationships with air temperature and soil temperature at 5 cm, 10 cm, 20 cm depths, and soil temperature at 5 cm depth was the most crucial influence factor among them. Meanwhile, temperature sensitivity (Q_{10}) of R_{eco} was negatively correlated with soil temperature. Light and temperature exerted strong controls over NEE and GPP. Aboveground biomass over the whole growing season showed non-linear relationships with CO_2 budget, while those during the early and peak growing season showed significant linear relationships with CO_2 budget. This research provides valuable reference for CO_2 exchange in estuarial saline wetland ecosystem.

Keywords: net ecosystem CO_2 exchange; ecosystem respiration; gross primary production; influencing factor; estuarial saline reed wetland; static chamber-GC method

Citation: Gao Manyu, Kong Fanlong, Xi Min, Li Yue, Li Jihua, 2017. Effects of environmental conditions and aboveground biomass on CO_2 budget in *Phragmites australis* wetland of Jiaozhou Bay, China. *Chinese Geographical Science*, 27(4): 539–551. doi: 10.1007/s11769-017-0886-6

1 Introduction

Recently, global warming caused by warming-greenhouse gas (GHG) emissions has drawn much attention due to its effect on rising sea level and causing frequent occurrence of extreme weather (Piao *et al*., 2003; Powell *et al*., 2006; Lee *et al*., 2015). As a GHG, CO_2 contributes 60% of global warming (Yang *et al*., 2015) and has increased steadily over the past century (IPCC, 2013). Therefore, CO_2 budget estimation and control mechanisms development are necessary (Fang *et al*., 2001; Batson *et al*., 2015; Lee *et al*., 2015).

Although only ~6% area of the Earth's surface is covered by wetlands (Strachan *et al*., 2015), wetlands store ~30% of terrestrial soil carbon (C) and thus play a critical role in global C cycle (Strachan *et al*., 2015). Therefore, it's vital to investigate CO_2 budget over different wetland ecosystems to accurately estimate global C budgets (Wickland *et al*., 2001; Bai *et al*., 2013; Zhao *et al*., 2016). Recently, most efforts have been focused

Received date: 2016-05-25; accepted date: 2016-09-22
Foundation item: Under the auspices of National Natural Science Foundation of China (No. 41101080), Shandong Natural Science Foundation of China (No.ZR2014DQ028, ZR2015DM004)
Corresponding author: XI Min. E-mail: ximin@qdu.edu.cn

on CO_2 flux (net ecosystem CO_2 exchange, NEE) (Syed *et al*., 2006; Han *et al*., 2014; Lee *et al*., 2015), CO_2 emission (ecosystem respiration, R_{eco}) (Fang *et al*., 1999; Ho *et al*., 2011; Xu *et al*., 2014), and their environmental influence factors (Hirota *et al*., 2006; Lindroth *et al*., 2007; Song and Liu, 2016). NEE and R_{eco} vary substantially in space and time, which respond to physical, chemical and biological characteristics of wetlands (Bonneville *et al*., 2008). For NEE, the overwhelming majority of wetlands act as long-term sinks for CO_2 (NEE < 0) (Bonneville *et al*., 2008; Strachan *et al*., 2015), only tiny minority of wetlands play contrary roles as long-term C sources (NEE > 0), such as the alpine wetland on the Qinghai-Tibet Plateau ecosystem in China (Zhang *et al*., 2008). On temporal scale, the seasonal NEE usually displays typical V-shaped distribution, which reaches its maximum value in July or August and then drops to the minimum in November or December (Han *et al*., 2013; Strachan *et al*., 2015; Yang *et al*., 2015). NEE can be influenced by several factors, such as light (Han *et al*., 2013; Lee *et al*., 2015), temperature (Lin *et al*., 2008; Lee *et al*., 2015) and biomass (Zhou *et al*., 2009; Han *et al*., 2013). Almost all wetlands release CO_2 (the value of R_{eco} was positive) in the dark chamber (Ho *et al*., 2011; Xu *et al*., 2014). R_{eco} in different seasons varied significantly (Xu *et al*., 2014; Song and Liu, 2016), because it was influenced by environmental conditions such as temperature (including soil temperature and air temperature) (Hirota *et al*., 2006; Song and Liu, 2016). For instance, Han *et al*. (2013) studied the R_{eco} over a reed wetland in the Yellow River Delta and concluded that variations of R_{eco} were well correlated with variations of soil temperature at 5 cm depth (r = 0.86) during the growing season. However, most efforts have been focused on NEE and R_{eco}, while limited studies have been carried out on quantification of NEE and R_{eco} and analysis of gross primary production (GPP), which represents CO_2 assimilation by photosynthesis of vegetation. Most efforts focused on environmental factors, when analyzing variable factors on CO_2 budget were investigated (Chen *et al*., 2015; Lee *et al.,* 2015; Wilson *et al*., 2015). Few studies were reported to determine the correlation between CO_2 budget and the botanical characteristics such as aboveground biomass of the vegetation covered in wetlands in different growing stages (Han *et al*., 2013; Song and Liu, 2016). Numerous researchers have applied themselves to CO_2 budget from peatlands (Maltby and Immirzi, 1993; Juszczak and Augustin, 2013) and floodplain wetlands (Samaritani *et al.*, 2013; Batson *et al.*, 2015). However, coastal wetlands are not well-documented by fieldwork owing to their harsh environmental condition (Morse *et al.*, 2012).

Estuarial saline wetland is considered to be one of the most productive ecosystems on the earth with the regular input of nutrients (Lee *et al*., 2015; Wang *et al*., 2016). As a vital type of coastal wetlands, estuarial saline wetland differs from other estuarial ecosystems since they are regularly inundated by tides (Ylva *et al*., 2011). Relatively small as the global estuarine area is, the CO_2 degassing flux in estuarine area is as large as the CO_2 uptake by the continental shelf (Lee *et al*., 2015). Thus, studying CO_2 budget in estuarial saline wetland timely is crucial for GHG control (Zhao *et al*., 2015; Song and Liu, 2016).

In the past decades, micrometeorological methods (eddy covariance technique, the Bowen ratio/energy balance method, the flux-gradient method, the aerodynamic method and others) (Baldocchi *et al.*, 1997; Kelliher *et al*., 1999; Zhou *et al.*, 2009; Lee *et al.*, 2015) and chamber methods (static chamber-gas chromatography (GC) method, dynamic chamber method and others) (Witkamp and Frank, 1969; Xu *et al*., 2014; Song and Liu, 2016) have been widely used to estimate CO_2 flux. The commonly applied methods among them were eddy covariance (EC) technique and static closed-GC method. There are large differences among all these methods in accuracy, spatial and temporal resolution, and applicability (Janssens *et al.*, 2000). Therefore, the choice of a specific technique is often a trade-off between requirements (accuracy and resolution) and feasibility (applicability and cost) (Janssens *et al*., 2000). In consideration of terrain, environment and experiment conditions in our study area, the static chamber-GC method was chosen to measure CO_2 flux.

In this study, we investigated NEE and R_{eco} simultaneously with 24h-measurement by applying static chamber-GC method and quantified GPP in accordance with the triadic relation among NEE, R_{eco} and GPP of estuarial saline *Phragmites australis* wetland in Jiaozhou Bay (JZB), a typical estuarial saline wetland in Shandong Province, China. Meanwhile, some influencing factors including air/soil temperature, illumination intensity and aboveground biomass were investigated to

determine their effects on CO_2 budget. The main purposes of this study were as follows: 1) quantify the CO_2 budget, including NEE, R_{eco} and GPP of the estuarial saline *P. australis* wetland in JZB; 2) determine the temporal variations of CO_2 budget; and 3) analyze the effects of air/soil temperature, illumination intensity and aboveground biomass on the dynamic of CO_2 budget.

2 Materials and Methods

2.1 Site description

Field experiment was conducted in the estuarial saline reed wetland (36°13′N, 120°06′E) along the riverbank of the Dagu River in JZB. This river is seasonal, whose wet season lasts from Jun to September, the normal flow season from October to January, and the dry season from February to May. *P.australis*, as a dominant species, widely exists near the Dagu River. The location of sampling site in this study was mapped in Fig. 1.

2.2 Gas sampling and flux quantifying

CO_2 fluxes were measured using static chamber-GC method. There are two kinds of chamber in this study, transparent chamber for measuring NEE and dark chamber for measuring ecosystem respiration. The sampling chamber included pedestal, lower chamber and upper chamber (Fig. 2). The pedestal was made by stainless steel, with a size of 70 cm × 70 cm × 20 cm. The lower and upper chambers were produced by stainless steel and organic glass, with the same size of 70 cm × 70 cm × 70 cm. The upper chamber contained a temperature sensor, a little fan and an air pressure balance tube. During sampling process, the pedestal was inserted into soil, while other parts of chamber were sealed by water to prevent air leakage. An insulating layer of sponge and aluminum foil was wrapped around the dark chamber to reduce the impact of direct radiative heating during sampling and minimize the air temperature changes inside the chamber. When the height of *P. austualis* was less than 70 cm, only the upper chamber was used to measure CO_2 fluxes. Both upper and lower chambers were chosen under the condition of plant height > 70 cm.

The gas sampling was conducted three times each month from May to October in 2014. Each sampling was collected at 6:00, 8:00, 10:00, 12:00, 14:00, 16:00, 18:00, 21:00, 0: 00 and 3:00 of the whole day. There are three repeats for the chamber measurement. Gas samples were manually extracted from the chamber with a 50-ml polypropylene syringe equipped with a three-way stopcock at 0, 10, 20 and 30 min after enclosure. Note that when light was strong, CO_2 concentration changed rapidly, so we adjusted the sampling time interval as 1 min. Thereafter, gas collection was injected into a

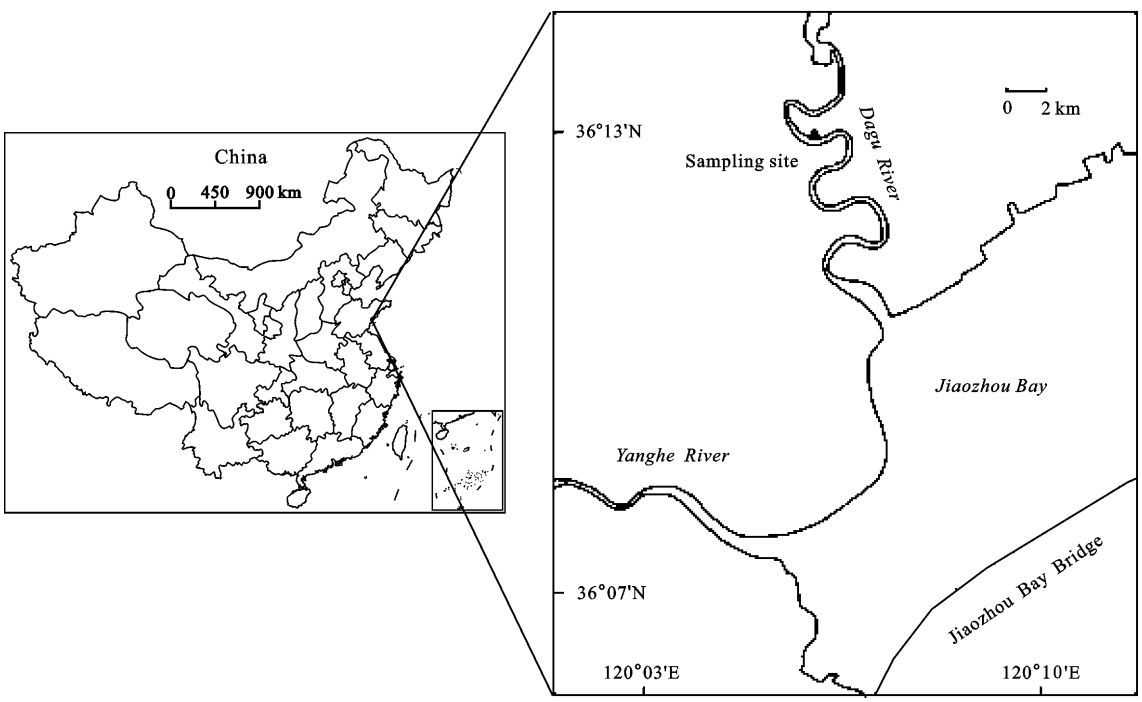

Fig. 1 Sketch of Jiaozhou Bay and sampling site

100 mL gas bag which had been pre-evacuated to approximately zero Pa and then stored in a dark cool box. The gas sampling was carried to the lab for CO_2 fluxes determination within 24 h.

Gas samples were analyzed using the gas chromatograph (GC-^{14}C, Shimadzu, Kyoto, Japan) with a thermal conductively detector (TCD). High-pure nitrogen was used as a carrier gas, at a flow rate of 30mL/min. The temperatures of the detector, column box, and injection port were 120℃, 50℃ and 100℃, respectively. CO_2 fluxes were calculated using the following equation (Yang *et al*., 2015):

$$F = H \times \frac{M}{V_0} \times \frac{P}{P_0} \times \frac{T_0}{T} \times \frac{\mathrm{d}C}{\mathrm{d}t} \quad (1)$$

where F is the gas flux (mg/(m^2·h)); H is the height (m) of chamber; M is the mole mass (mg/mol) of CO_2; P is the atmospheric pressure (kPa) at the sampling site; T is the absolute temperature (K) during sampling; V_0, P_0 and T_0 are the gas mole volume (m^3/mol), air atmospheric pressure (kPa) and air absolute temperate (K) under standard conditions respectively; dC/dt is the slope of the gas concentration curve variation along with time t (h).

NEE and R_{eco} were respectively measured by the transparent chamber-GC and dark chamber-GC methods, and calculated by the above equation. GPP represents CO_2 assimilation by photosynthesis of vegetation (Han *et al*., 2013). It was obtained using the following equation (Han *et al*., 2013):

$$GPP = R_{eco} - NEE \quad (2)$$

2.3 Determination of illumination intensity, air temperature and soil temperature

The illumination intensity was determined by using illuminometer (TES-1332A). Air temperature was obtained from the temperature sensor inside the upper chamber. Soil temperatures at different depths (5 cm, 10 cm and 20 cm) were measured by thermometers.

2.4 Determination of aboveground biomass

During the growing period, aboveground biomass (AGB) of reed was also measured. Three sampling points were randomly chosen with the individual area of 0.25 m^2 (0.5 m × 0.5 m). The aboveground parts of *P. austualis* were collected. All plant samples were firstly dried at 105℃ for one hour and then dried at 80℃ for 48h to get their dry weight (DW). AGB was calculated using the following equation:

$$AGB = \frac{DW}{S} \quad (3)$$

Where DW and S represent plant dry weight (g) and plot area (m^2), respectively.

3 Results

3.1 Temporal variations of CO_2 budget

Figure 3 shows the diurnal variations of NEE, R_{eco} and GPP during the targeted experimental period from May to October in 2014. Apparently, diurnal variations of NEE among different months were similar, and exhibited a significant V-like pattern during daytime (6:00 to

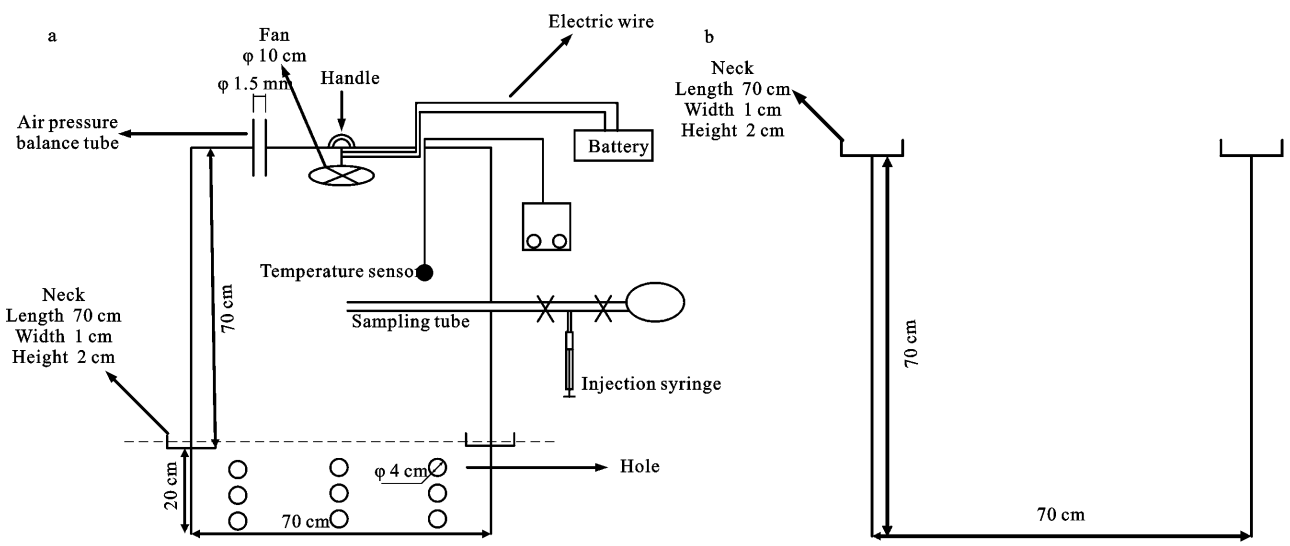

Fig. 2 Design drawing of static chamber including pedestal, upper chamber (a) and lower chamber (b)

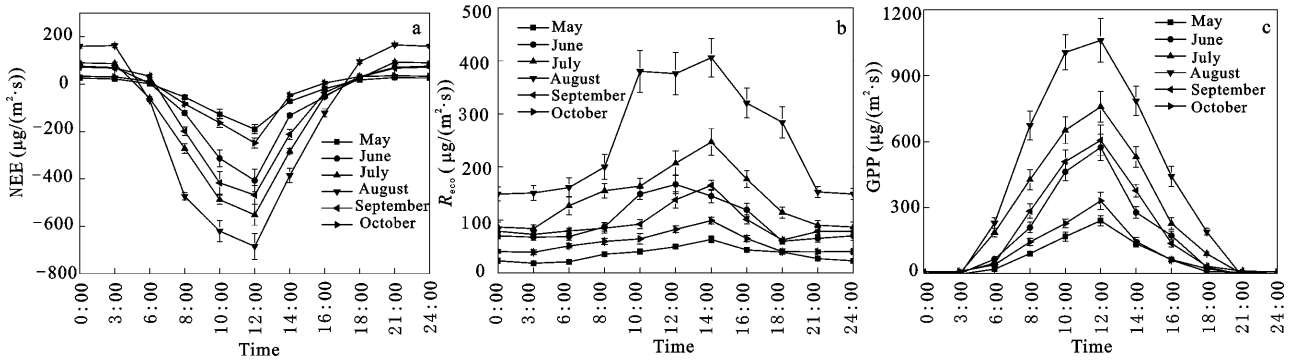

Fig. 3 Diurnalvariations of net ecosystem exchange (NEE) (a), ecosystem respiration (R_{eco}) (b), and gross primary production (GPP) (c) from May to October in 2014. Vertical bars show standard deviation (n = 3)

18:00). The minimum values appeared at 12:00. At daytime, the NEE values were negative, which suggested that the ecosystem acted as a CO_2 sink. At night, the NEE values were higher than zero, indicating that the ecosystem acted as a CO_2 source. Meanwhile, R_{eco} increased forenoon and then decreased after 14:00. The measured maximum R_{eco} value (400.28 μg/(m^2·s)) is obtained in August. During the daytime, GPP increased firstly and reached the peak at 12:00; then it exhibited a decreasing tendency. The size order of GPP was in the following order: August > July > September > June > October > May.

The monthly variations of NEE, R_{eco} and GPP are shown in Fig. 4a. As revealed, NEE decreased slightly at first from May to August and then regrew from August to October. It can be observed that the maximum and minimum NEE appeared in August (–11.08 g/(m^2·d)) and October (–2.33 g/(m^2·d)), respectively. Meanwhile, R_{eco} and GPP showed opposite trend with NEE, increasing from May to August and then decreased. The maximum values of R_{eco} and GPP appeared in August. R_{eco}/GPP is commonly applied to evaluate the relative contribution of carbon exchange processes (respiration and photosynthesis) to total exchange (Falge *et al*., 2001). Fig. 4b depicts monthly variations of R_{eco}/GPP, which ranged from 0.53 to 0.67. Moreover, the ratio values in June, September and October were significantly higher than those in other three months. The cumulative value of NEE, R_{eco} and GPP were 1129.16 g/m^2, 1744.89 g/m^2 and 2874.05 g/m^2 during the entire growing season.

3.2 Environmentalconditions and aboveground biomass

Figure 5 shows the monthly variations of illumination intensity, temperature and aboveground biomass. The range of illumination intensity was 24 740 lux to 51 457 lux. Air temperature ranged from 18.6℃ to 24.5℃. Meanwhile, the variations of soil temperature in different depths at 5 cm, 10 cm and 20 cm were similar but different from air temperature. For example, the soil temperature was approximately 17℃ in May, when the air temperature was 19℃ at the same time. Monthly aboveground biomass of reed increased gradually through the growing season till a peak (2245.14 g/m^2) was observed in September.

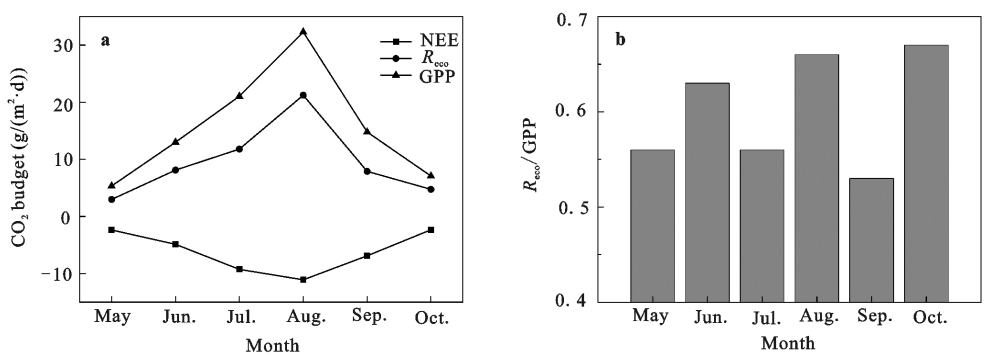

Fig. 4 Monthly variations of NEE, R_{eco}, and GPP from May to October in 2014 (a) and ratio of R_{eco} to GPP from May to October in 2014 (b)

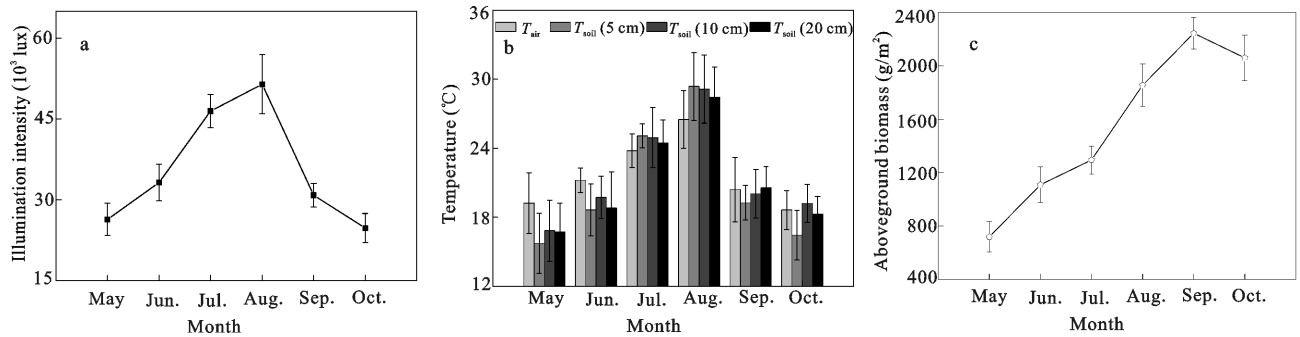

Fig. 5 Seasonal variations of illumination intensity (a), air temperature (T_{air}) and soil temperature (T_{soil}) at 5 cm, 10 cm, and 20 cm depths (b), and aboveground biomass (c) from May to October in 2014. Vertical bars show standard deviation (n = 3)

3.3 Relationships between CO_2 budget and environmental conditions as well as aboveground biomass

Regression analysis was used to analyze the relationships between R_{eco} and air/soil temperature. Generally, R_{eco} fitted well with temperature no matter air temperature or soil temperature at different depths ($R^2 > 0.6$) (Fig. 6) and the R^2 of R_{eco} and soil temperature at 5 cm depth was the largest one, which indicated that soil temperature at 5 cm depth was a more important influence factor to R_{eco} compared with air temperature and soil temperature at 10 cm or 20 cm depths. Meanwhile, both NEE and GPP were significantly related to illumination intensity (Fig. 7), revealing exponential relationships. Besides, correlation analysis indicated that NEE and GPP correlated significantly with temperature variations (Table 1); both NEE and GPP were more obviously related to air temperature. To be specific, they had exponential relationships (R^2 equaled 0.45 and 0.69, respectively) (Fig. 8). During the entire growing season, CO_2 budget showed polynomial relationships with AGB, which accounted for variation in NEE, R_{eco} and GPP of 45%, 57% and 51%, respectively. During the early and peak growing season (May to August), CO_2 budget was strongly correlated with the temporal variation of AGB, revealing significant linear correlations, and the changes in AGB could explain 84%–90% of the monthly variations in CO_2 budget (Fig. 9)

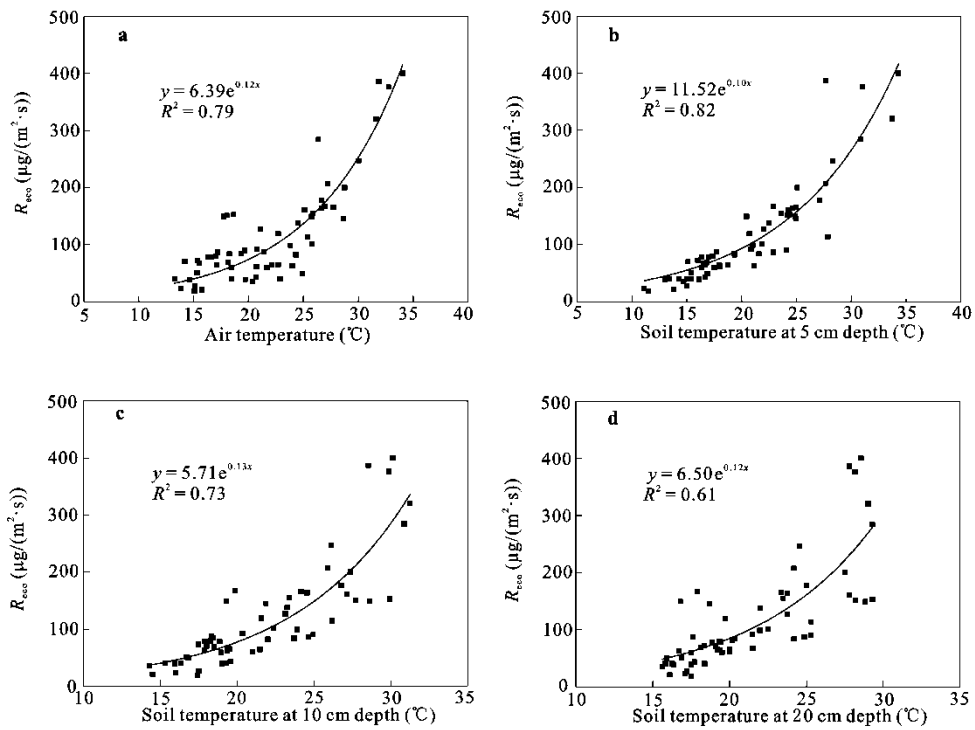

Fig. 6 Relationships of R_{eco} with air temperature (a), soil temperature at different depths of 5 cm (b), 10 cm (c), and 20 cm (d)

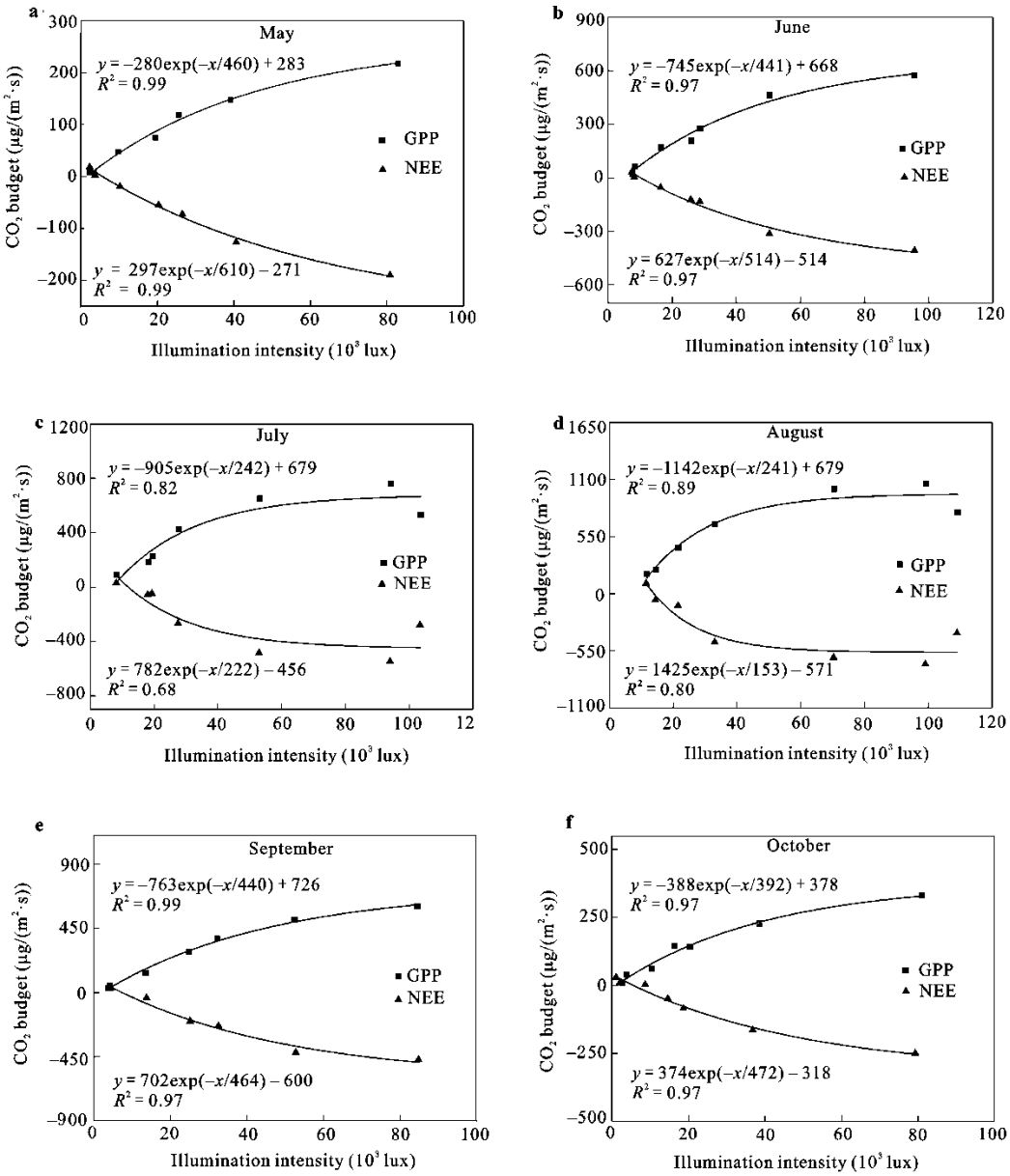

Fig. 7 Relationships between CO_2 budgets (NEE, GPP) and illumination intensity from May to October in 2014

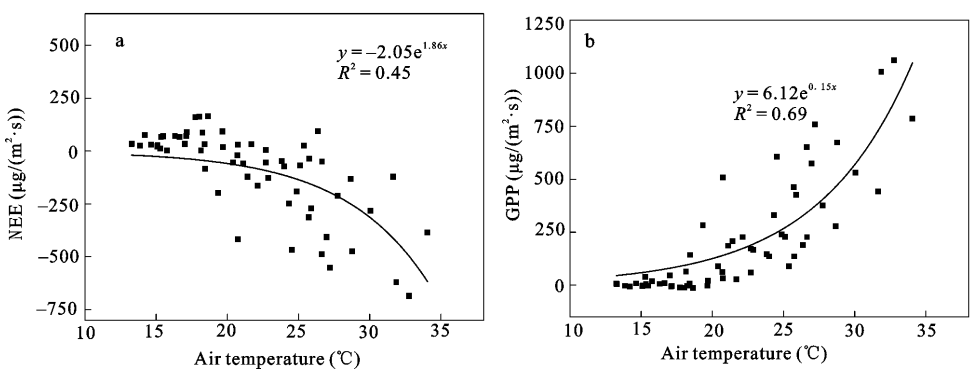

Fig. 8 Relationship between NEE and air temperature (a), and relationship between GPP and air temperature (b)

Table 1 Correlation coefficients of daytimenet ecosystem CO_2 exchange (NEE) and daytime gross primary production (GPP) with air and soil temperature during growing season in reed wetland of Jiaozhou Bay

CO_2 budget ($\mu g/(m^2 \cdot s)$)	Temperature(℃)			
	Air	5-cm soil	10-cm soil	20-cm soil
NEE	–0.723**	–0.412**	–0.298*	–0.219
GPP	0.820**	0.603**	0.503**	0.425**

Notes: $^{**}P < 0.01$; $^{*}P < 0.05$

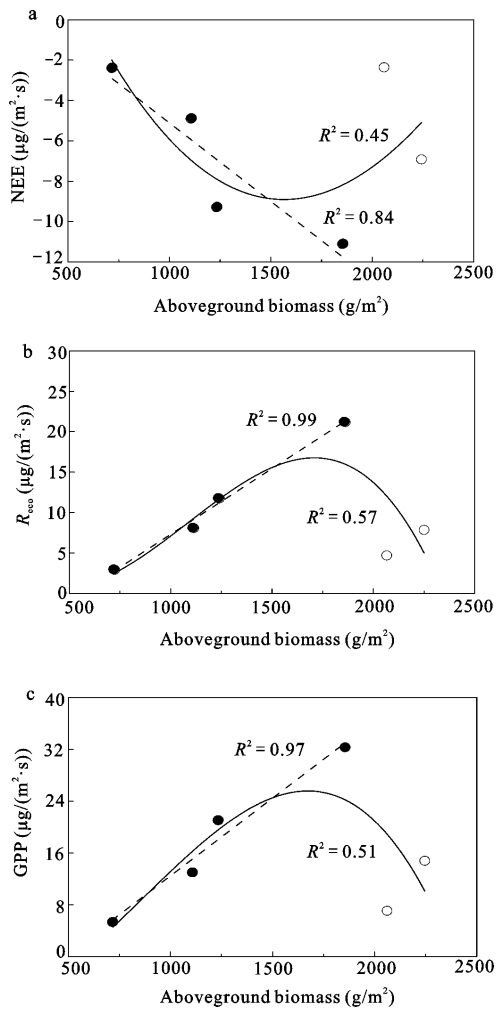

● During early and peak growing season (May to August); ○ During later growing season (September and October); —Linear fit during early and peak growing season; ---Polynomial fit during entire growing season

Fig. 9 Relationships between CO_2 budget (NEE, R_{eco} and GPP) and aboveground biomass of reed in wetland from May to October in 2014

4 Discussion

4.1 CO_2 budget in response to temperature and illumination intensity

4.1.1 R_{eco} in response to temperature

Variations of air and soil temperatures are the dominant factors which affect the value of R_{eco} (Powell *et al.*, 2006). There were two possible reasons to explain that R_{eco} fitted well with temperature: on one hand, higher temperature could promote microbial respiration by activating dormant microbes and increasing microbial species richness (Andrews *et al.*, 2000); on the other hand, the rates of the enzymatic processes of respiration could become larger with the increasing temperature (Ryan, 1991). It was worth noting that when compared with air temperature and soil temperature at 10 cm or 20 cm depths, soil temperature at 5 cm depth was a more important influence factor to R_{eco} in our study. This result was in accordance with results obtained by Alberto *et al*. (2009), Schedlbauer *et al*. (2010) and Han *et al*. (2014).

Q_{10}, an indicator of temperature sensitivity, is defined as the factor in the rate increases by 10℃ (Van't Hoff, 1898), which has been commonly used to express the impact of temperature on R_{eco}. It can be estimated as the following equation:

$$Q_{10}=\exp\ (10b) \tag{4}$$

Where b is regression coefficient of the regression model of the relationship between R_{eco} and soil temperature at a certain depth (Xu and Qi, 2001). In this study, the values of Q_{10} based on soil temperature at 5 cm depths was calculated as 2.86 during the whole growing season. It has been proved that Q_{10} was significantly influenced by soil temperature (Xu and Qi, 2001; Gershenson *et al*., 2009). To further illustrate the effect of soil temperature on Q_{10}, R_{eco} were separated into four classes (Table 2). The result revealed that soil temperature was negatively correlated with Q_{10} values, companied by the appearance of highest Q_{10} at the lowest temperature conditions ($T_{soil} \leq 15$℃). This negative correlation between Q_{10} and temperature observed in our study was consistent with previous studies (Xu and Qi, 2001; Gershenson *et al*., 2009). For example, Xu and Qi (2001) reported that Q_{10} evidently declined with increases in soil temperature and found a simple linear regression model explaining 45% of the variation of Q_{10} values. The mechanisms responsible for higher Q_{10} occurring at a lower soil temperature level were complicated. To be specific, soil temperature can directly impact the Q_{10} value of ecosystem respiration by affecting enzyme activity taken part in the reaction, root growth and microorganism accumulation, thereby affecting Q_{10}

Table 2 Relationships between R_{eco} and soil temperature (T_{soil}) at 5 cm depth and corresponding Q_{10} under different temperature classes in reed wetland from May to October in 2014

Temperature class	Respiration-temperature relationship	*n*	R^2	Q_{10}
≤15℃	$y=3.66e^{0.159x}$	8	0.45	4.90
15℃< T_{soil} ≤20℃	$y=6.17e^{0.135x}$	22	0.38	3.86
20℃ <T_{soil} ≤2℃	$y=12.22e^{0.101x}$	21	0.34	2.75
≥25℃	$y=20.92e^{0.085x}$	11	0.45	2.34

Notes: y represents ecosystem respiration (μg/(m^2·s)), x represents soil temperature at 5 cm depth (℃)

values (Yang *et al*., 2011). Meanwhile, soil temperature directly impacts the substrate availability and substrate quality and indirectly affects Q_{10}. A small deviation of Q_{10} may cause a significant bias in estimating soil respiration because of the nonlinear relationship between Q_{10} and respiration (Xu and Qi, 2001). Therefore, characterizing of Q_{10} and its variation is of vital importance to estimate ecosystem carbon balance and its uncertainty bounds (Xu and Qi, 2001).

4.1.2 NEE and GPP in response to illumination intensity and temperature

It has been proved that illumination was the dominate factor for NEE and GPP control (Powell *et al*., 2006; Lindroth *et al*., 2007; Lee *et al*., 2015). NEE and GPP revealed strong exponential relationships with illumination intensity (Fig. 7). The correlations of illumination intensity to NEE and GPP were relatively poor during July and August compared with those in other months. The difference could be explained by the following different rules of NEE and GPP changes with illumination intensity in different months. At the outset, the absolute magnitudes of NEE and GPP increased fast (Fig. 7); then as illumination intensity reached a certain level, NEE and GPP began to keep steady. Threshold value of illumination intensity is called illumination saturation point, which is related to environmental conditions such as temperature (Yang *et al*., 2013). Moreover, the absolute values of NEE and GPP trended down when illumination intensity was high enough in July and August, suggesting a photo inhibition of photosynthesis appearing in the ecosystem under high temperature and intense radiation conditions (Wu *et al*., 2010). The decrease of NEE and GPP absolute values indicated that the photosynthetic capacity and light use efficiency decreased (Han *et al*., 2013). Overall, the rate of daytime GPP change with the changing illumination intensity was slightly faster than the rate of daytime NEE change, in accordance with the observation of Wu *et al*. (2010).

However, ecosystem photosynthetic capacity in different growth stage could also be affected by changes in air and soil temperature (Lafleur *et al*., 2001; Zhang *et al*., 2006). Our findings of the relationships between temperature and NEE, GPP were in agreement with the findings of previous studies (Zhang *et al*., 2006; Lee *et al*., 2015). Moreover, Lin *et al*. (2008) reported that under the same illumination intensity, the ecosystem photosynthetic rate usually increased with temperature. Meanwhile, Wu *et al*. (2010) divided NEE and GPP into two groups, which were studied in the morning and in the afternoon respectively. The rate of daytime NEE change was lower than that of GPP change. Under the same light conditions, the above phenomenon was observed to be more distinct in the afternoon, indicating that the increase of temperature could enhance the capacity of ecosystem photosynthesis. In conclusion, NEE and GPP during the daytime were co-determined by light and temperature.

4.2 CO_2 budget in response to aboveground biomass

Researchers suggested that CO_2 budget were well correlated with aboveground living biomass of vegetation (Han *et al*., 2013; Song and Liu, 2016). However, our result that CO_2 budget showed polynomial relationships with AGB during the entire growing season was disagreed with those in some other researches which found that NEE, R_{eco} and GPP revealed significant linear correlations with AGB (Hirota *et al*., 2006; Han *et al*., 2013). Therefore, to further investigate the effects of AGB on CO_2 budget, the monthly CO_2 budget data were separated into two groups over two growth periods: the early and peak growing season (from May to August) and the later growing season (September and October). Specifically, during the early and peak growing season, CO_2 budget was strongly correlated on the temporal variation of AGB (Fig. 9). The difference of these results may due to the following reasons: with the decrease of temperature and illumination intensity, the absolute magnitude of CO_2 budget during the later growing season dropped to a low level even with higher AGB. In addition, as the community senesced and the reed growth arrested, the growth rate and metabolism rate of reed slowed down, causing the decline of reed

CO_2 budget. Specifically, leaf grew fast and became the main part of AGB in the vegetation stage. The decrease of leaf weight and leaf area could lead to a decline in photosynthesis even under a rise in AGB during the later growing season. Hence CO_2 budget negatively correlated with AGB during the later growing season. In a word, the temporal variation in AGB had a great impact on NEE, R_{eco} and GPP.

Combined with previous researches, the aboveground biomass of vegetation may exert impact on CO_2 exchange via the following tips. First and foremost, to some extent, AGB was associated with photosynthetic capacity of living plant (Han *et al*., 2013), therefore NEE was modulated by the amount of plant biomass (Larmola *et al*., 2003). Secondly, it was a good proxy for living plant AGB to explain the variation of respiration in both autotrophic and heterotrophic capacity and therefore the variation in AGB regulated the variability in R_{eco} (Wohlfahrt *et al*., 2008). Last but not least, AGB was relevant to leaf area index (Wickland *et al*., 2001), which could impact photosynthetic CO_2 uptake by controlling ecosystem light absorption capacity (Lund *et al*., 2010).

4.3 Comparison of CO_2 budget with other wetland ecosystems

In this study, diurnal variations of NEE among different months in the growing season exhibited significant V-like patterns during daytime; meanwhile seasonal variations of CO_2 budget showed single peak curves from May to October. Same results have been reported by previous researchers (Syed *et al*., 2006; Han *et al*., 2014; Lee *et al*., 2015). In complete length of the growing season, the net CO_2 uptake of the reed wetland was 1129.16 g/m^2, greater than most studies (Han *et al*., 2013; Yang *et al*., 2013; Strachan *et al*., 2015) (Table 3), suggesting that the coastal wetland in JZB was an area with better ability of carbon sequestration during the reed growing season.

Furthermore, the average ratio of R_{eco} to GPP in our study area was 0.61 during the growing season, which was equal to a reed wetland in the Yellow River Delta in China (0.61) (Yang *et al*., 2013) and much lower than Cattail marsh in the Ottawa River Valley in Canada (0.88) (Strachan *et al*., 2015) (Table 3). Overall, the ratio of R_{eco} to GPP was intermediate. Besides, the ratio of R_{eco} to GPP reached its maximum in October and minimum in May, which was inconsistent with results observed by Han *et al*. (2013) that the highest R_{eco}/GPP value achieved in May. The differences may probably due to the lowest illumination intensity in October among the six months, causing a relatively low rate of photosynthesis. Meanwhile, soil temperature at 5 cm depth in October was higher than that in May, resulting in stronger respiration. Therefore, the maximum value of R_{eco}/GPP was appeared in October instead of May.

5 Conclusions

The estuarial saline reed (*P. australis*) wetland in JZB acted as a CO_2 sink of 1129.16 g/m^2 in the entire growing season (May to October). The cumulative value of R_{eco} and GPP were 1744.89 g/m^2 and 2874.05 g/m^2 respectively; the ratio of R_{eco} and GPP was 0.61. CO_2 budget showed distinct diurnal and seasonal patterns. Seasonal variation of CO_2 budget exhibited single peak curves in the growing season. R_{eco} was significantly related to air temperature and soil temperature, especially at 5 cm depth. Q_{10} values were negatively related to soil temperatures. Both NEE and GPP were significantly

Table 3 Comparison of CO_2 budget (NEE, R_{eco} and GPP) and R_{eco}/GPP in different ecosystems during vegetation growing season

Location	Ecosystem	NEE(g/m^2)	R_{eco}(g/m^2)	GPP(g/m^2)	R_{eco}/GPP	Observation time	Reference
Yellow River Delta, China	Reed wetland	–956	1657	2612	0.63	May–October 2010	Han *et al*., 2013
Yellow River Delta, China	Reed wetland	–781	1242	2023	0.61	May–October 2011	Yang *et al*., 2013
Qinghai-Tibet Plateau, China	Alpine herb wetland	–230	1735	1965	0.88	May–September 2005	Zhang *et a*l., 2008
Ottawa River Valley, Canada	Cattail marsh	–64	468	532	0.88	May–September 2010	Strachan, *et al*., 2015
Mexico Estuary, America	Cladiumjamaicense tidal freshwater marsh	–825	1286	2111	0.61	May–October 2012	Wilson *et al*., 2015
Boreal Forest Natural Region, Canada	Peatland	–154	–	–	–	May–October 2005	Adkinson *et a*l., 2011
Jiaozhou Bay, China	Coastal saltmarsh reed wetland	–1129	1745	2874	0.61	May–October 2014	This study

related to illumination intensity and temperature. Aboveground biomass over the whole growing season revealed nonlinear relationships with CO_2 budget, while AGB during the early and peak growing season showed significant linear relationships with CO_2 budget.

Acknowledgements

The authors thank the students from Qingdao University for helping with lab experiments.

References

Adkinson A C, Syed K H, Flanagan L B, 2011.Contrasting responses of growing season ecosystem CO_2 exchange to variation intemperature and water table. *Journal Geophysical Research*, 116(G1): 99–112. doi: 10.1029/2010JG001512

Alberto M C R, Wassmann R, Hirano T *et al*., 2009. CO_2 heat fluxes in rice fields: comparative assessment of flooded and non-flooded fields in the Philippines. *Agriculture and Forest Meteorology*, 149(10): 1737–1750. doi: 10.1016/j.agrformet.2009.06.003

Andrews J A, Matamala R, Westover KM *et al*., 2000. Temperature effects on the diversity of soil heterotrophs and the $\delta^{13}C$ of soil-respired CO_2. *Soil Biology Biochemistry*, 32(32): 699–706. doi: 10.1016/S0038-0717(99)00206-0

Bai J H, Cui B S, Cao H C *et al*., 2013. Wetland degradation and ecological restoration. *The Scientific Word Journal.* (3): 523–632. doi: org/10.1155/2013/523632

Baldocchi D D, Vogel C A and Hall B, 1997. Seasonal variation of carbon dioxide exchange rates above and below a boreal jack pine forest. *Agriculture and Forest Meteorology*, 83(1): 147–170.

Batson J, Noe G B, Hupp C R *et al*., 2015. Soil greenhouse gas emissions and carbon budgeting in a short-hydroperiod floodplain wetland. *Journal of Geophysical Research*: *Biogeosciences*, 120(1): 77–95. doi: 10.1002/ 2014JG002817

Bonneville M C, Strachan I B, Humphreys E R *et al*., 2008.Net ecosystem CO_2 exchange in a temperate cattail marsh in relation to biophysical properties. *Agricultural and Forest Meteorology*, 148(1): 69–81. doi: 10.1016/j.agrformet.2007.09.004

Chen Y P, Chen G C, Ye Y, 2015. Coastal vegetation invasion increases greenhouse gas emission from wetland soils but also increases soil carbon accumulation. *Science of the Total Environment*, 526:19–28. doi: 10.1016/j.scitotenv.2015.04.077

Gershenson A, Bader N E, Cheng W X, 2009. Effects of substrate availability on the temperature sensitivity of soil organic matter decomposition. *Global Change Biology*, 15(1): 176–183. doi: 10.1111/j.1365-2486.2008.01827.x

Fang J Y, Tang Y H, Koizumi H *et al*., 1999. Evidence of wintertime CO_2 emission from snow-covered grounds in high latitudes. *Science in China* (*Series D*), 42(4): 378–382.

Fang Jingyun, Piao Shilong, Zhao Shuqing, 2001. The carbon sink: the role of the middle and high latitudes terrestrial ecosystems in the northern hemisphere. *Acta Phytoecologica Sinica*, 25(5): 594–602. (in Chinese)

Falge E, Baldocchi D, Olson R J *et al*., 2001. Gap filling strategies for defensible annual sums of net ecosystem exchange. *Agricultural and Forest Meteorology*, 107(1): 43–69. doi: 10.1016/S0168-1923(00)0022-2

Guo X, Dai M, Zhai W *et al*., 2009. CO_2 flux and seasonal variability in a large subtropical estuarine system, the Pearl River Estuary, China. *Journal of Geophysical Research*, 114(G3): 5283–5288. doi: 10.1029/2008JG000905

Han G X, Xing Q H, Yu J B *et al*., 2014. Agricultural reclamation effects on ecosystem CO_2 exchange of a coastal wetland in the Yellow River Delta. *Agriculture*, *Ecosystems and Environment*, 196(1793): 187–198. doi: 10.1016/j.agee.2013.09.012

Han G X, Yang L Q, Yu J B *et al*., 2013. Environmental controls on net ecosystem CO_2 exchange over a reed (*Phtagmites australis*) wetland in the Yellow River Delta, China. *Estuaries and Coasts*, 36(2): 401–413. doi: 10.1007/s12237-012-9572-1

Hirota M, Tang Y H, Hu Q W, 2006. Carbon dioxide dynamics and controls in a deep-water wetland on the Qinghai-Tibetan Plateau. *Ecosystems*, 9(4): 673–688. doi: 10.1007/s10021–006-0029-x

Ho S H, Chen C Y, Lee D J *et al*., 2011. Perspectives on microalgal CO_2 emission mitigation systems–A review. *Biotechnology Advances*, 29(2): 189–198. doi: 10.1016/j.biotechadv.2010.11.001

IPCC (Intergovernmental Panel on Climate Change), 2013. Impacts, adaptation, and vulnerability. In: Stocker T F *et al*. (eds.). *The Physical Science Basis. Contribution of Working Group I to the Fifth Assessment Report of the Intergovernmental Panel on Climate Change*. Cambridge: Cambridge University Press.

Janssens I A, Kowalski A S, Longdoz B *et al*., 2000.Assessing forest soil CO_2 efflux: an in situ comparison of four techniques. *Tree Physiology*, 20(1): 23–32.

Juszczak R, Augustin J, 2013. Exchange of the greenhouse gases methane and nitrous oxide between the atmosphere and a temperate peatland in central Europe. *Wetlands*, 33(5): 895–907. doi: 10.1007/s13157-013-0448-3

Kelliher F M, Lloyd J, Arneth A *et al*., 1999. Carbon dioxide efflux density from the floor of a central Siberian pine forest. *Agriculture and Forest Meteorology*, 93(3–4): 217–232.

Lafleur P M, Roulet N T, Admiral S W, 2001. Annual cycle of CO_2 exchange at a bog peatland. *Journal of Geophysical Research Atmospheres*, 106(D3): 3071–3081. doi: 10.1029/2000JD900588

Larmola T, Alm J, Juutinen S *et al*., 2003. Ecosystem CO_2 exchange and plant biomass in the littoral zone of a boreal eutrophic lake. *Freshwater Biology*, 48(8): 1295–1310.doi: 10.1046/j.1365-2427.2003.01079.x

Lee C, Fan C J, Wu Z Y *et al*., 2015. Investigating effect of environmental controls on dynamics of CO_2 budget in a subtropical estuarial marsh wetland ecosystem. *Environmental Research Letters*, 10(2): 25005–25016. doi: 10.1088/1748-9326/

10/2/025005

Lindroth A, Lund M, Nilsson M *et al*., 2007. Environmental controls on the CO_2 exchange in north European mires. *Tellus Series B-chemical and Physical Meteorology*, 59(5): 812–825. doi: 10.1111/j.1600-0889.2007.00310.x

Lin Dong, Lü Shihai, Feng Chaoyang *et al*., 2008. Grass-shrub vegetation response to change of CO_2 concentration and temperature in the mountains of north China. *Pratacultural Science*, 25(4): 135–140. (in Chinese)

Lloyd J, Taylor J A, 1994. On the temperature dependence of soil respiration. *Functional Ecology*, 8(3): 315–323. doi: 10.2307/2389824

Lund M, Lafleur P M, Roulet N T *et al*., 2010. Variability in exchange of CO_2 across 12 northern peatland and tundra sites. *Global Change Biology*, 16(9): 2436–2448. doi: 10.1111/j.1365-2486.2009.02104.x

Maltby E, Immirzi P, 1993. Carbon dynamics in peatlands and other wetland soils regional and global perspectives. *Chemosphere*, 27(6): 999–1023. doi: 10.1016/0045–6535(93)90065–D

Morse J L, Ardon M, Bernhardt E S, 2012. Greenhouse gas fluxes in southeastern U.S. coastal plain wetlands under contrasting land uses. *Ecological Applications*, 22(1): 64–280. doi: 10.1890/11–0527.1

Piao S L, Fang J Y, Chen A P, 2003. Seasonal dynamics of terrestrial net primary production in response to climate changes in China. *Acta Botanica Sinica*, 45(3): 269–275.

Powell T L, Bracho R, Li J H *et al*., 2006. Environmental controls over net ecosystem carbon exchange of scrub oak in central Florida. *Agricultural and Forest Meteorology*, 141(1): 19–34. doi: 10.1016/j.agrformet.2006.09.002

Ryan M G, 1991. Effects of climate change on plant respiration. *Ecological Applications*, 1(2): 157–167.doi: 10.2307/1941808

Samaritani E, Shrestha J, Fournier B *et al*., 2013. Heterogeneity of soil carbon pools and fluxes in a channelized and a restored flood plain section (Thur River, Switzerland). *Hydrology and Earth System Sciences*, 15(6): 1757–1769. doi: 10.5194/hess-15-1757-2011

Schedlbauer J L, Oberbauer S F, Starr G *et al*., 2010. Seasonal differences in the CO_2 exchange of a short-hydroperiod Florida Everglades marsh. *Agricultural and Forest Meteorology*, 150(7–8): 994–1006. doi: 10.1016/j.agrformet.2010.03.005

Song H L, Liu X T, 2016. Anthropogenic effects on fluxes of ecosystem respiration and methane in the Yellow River estuary, China. *Wetlands*, 36(1): S113–S123. doi: 10.1007/s13157-014-0587-1

Strachan I B, Nugent K A, Crombie S *et al*., 2015. Carbon dioxide and methane exchange at a cool-temperate fresh water marsh. *Environmental Research Letters*, 10(6): 65006–65015. doi: 10.1088/1748-9326/10/6/065006

Syed K H, Flanagan L B, Carlson P J *et al*., 2006. Environmental control of net ecosystem CO_2 exchange in a treed, moderately rich fen in northern Alberta. *Agricultural and Forest Meteorology*, 140(1–4): 97–114. doi: 10.1016/j.agrformet.2006.03.022

Van't Hoff J H, 1898. *Lectures on Theoretical and Physical Chemistry*. London: Edward Arnold Press.

Wang J J, Bai J H, Zhao Q Q *et al*., 2016. Five-year changes in soil organic carbon and total nitrogen in riparian wetlands affected by flow-sediment regulation in a Chinese delta. *Scientific Reports*. doi: 10.1038/srep21137

Wickland K, Striegl R, Mast M *et al*., 2001. Carbon gas exchange at a southern Rocky Mountain wetland, 1996–1998. *Global Biogeochemical Cycle*s, 15(2): 321–335. doi: 10.1029/2000GB001325

Wilson B J, Mortazavi B, Kiene R P, 2015. Spatial and temporal variability in carbon dioxide and methane exchange at three coastal marshes along a salinity gradient in a northern Gulf of Mexico estuary. *Biogeochemistry*, 123(3): 329–347. doi: 10.1007/s10533-015-0085-4

Witkamp M, Frank M L, 1969. Evolution of CO_2 from litter, humus and subsoil of a pine stand. *Pedobiologia*, 9(5–6): 358–365.

Wohlfahrt G, Anderson-Dunn M, Bahn M *et al*., 2008. Biotic, abiotic, and management controls on the net ecosystem CO_2 exchange of European mountain grassland ecosystems. *Ecosystems*, 11(8): 1338–1351. doi: 10.1007/s10021-008-9196-2

Wu Libo, Gu Song, Zhao Liang *et al*., 2010. Variation in net CO_2 exchange, gross primary production and its affecting factors in the planted pasture ecosystem in Sanjiang Yuan Region of the Qinghai-Tibetan Plateau of China. *Chinese Journal of Plant Ecology*, 34(7): 770–780. (in Chinese)

Xu M, Qi Y, 2001. Spatial and seasonal variations of Q_{10} determined by soil respiration measurements at a Sierra Nevadan forest. *Global Biogeochemical Cycles*, 159(3): 687–696. doi: 10.1029/2000GB001365

Xu W H, Zou X Q, Cao L G *et al*., 2014. Seasonal and spatial dynamics of greenhouse gas emissions under various vegetation covers in a coastal saline wetland in southeast China. *Ecological Engineering*, 73(2014): 469–477. doi: 10.1016/j.ecoleng.2014.09.087

Yang Liqiong, Han Guangxuan,Yu Junbao *et al*., 2013. Net ecosystem CO_2 exchange and its environmental regulation mechanisms in a reed wetland in the Yellow River Delta of China during the growth season. *Chinese Journal of Applied Ecology*, 24(9): 2415–2422. (in Chinese)

Yang P, He Q H, Huang J F *et al*., 2015. Fluxes of greenhouse gases at two different aquaculture ponds in the coastal saline wetland in southeast China. *Ecological Engineering*, 115(2015): 269–277. doi: 10.1016/j.atmosenv.2015.05.067

Yang Qingpeng, Xu Ming, Liu Hongsheng, 2011. Impact factors and uncertainties of the temperature sensitivity of soil respiration. *Acta Ecologica Sinica*, 31(8): 2301–2311. (in Chinese)

Ylva S O, Armel D, Angus G *et al*., 2011. Cattle grazing drives nitrogen and carbon cycling in a temperate salt marsh. *Soil Biology and Biochemistry*, 43(3): 531–541. doi: 10.1016/j.soilbio.2010.11.018

Zhang Fawei, Liu Anhua, Li Yingnian *et al*., 2008. CO_2 flux in alpine wetland ecosystem on the Qinghai–Tibetan Plateau. *Acta Ecologica Sinica*, 28(2): 453–462. (in Chinese)

Zhang L M, Yu G R, Sun X M *et al*., 2006. Seasonal variations of

ecosystem apparent quantum yield (alpha) and maximum photosynthesis rate (P-max) of different forest ecosystems in China. *Agricultural & Forest Meteorology*, 137(3–4): 176–187. doi: 10.1016/j.agrformet.2006.02.006

Zhao Q Q, Bai J H, Liu Q *et al*., 2015. Decomposition and carbon and nitrogen dynamics of *Phragmites australis* litter as affected by flooding periods in coastal wetlands. *Clean-Soil Air Water*, 43(3): 441–554. doi: 10.1002/clen.201300823

Zhao Q Q, Bai J H, Liu Q *et al.*, 2016. Spatial and seasonal variation of soil carbon and nitrogen content and stock in a tidal salt marsh with *Tamarix chinensis*, China. *Wetlands*, 36(Suppl1): S145–S152. doi: 10.1007/s13157-015-0647-1

Zhou L, Zhou G S, Jia Q Y, 2009. Annual cycle of CO_2 exchange over a reed (*Phragmites australis*) wetland in Northeast China. *Aquatic Botany*, 91(91): 91–98. doi: 10.1016/j.aquabot.2009.03.002